Renewable Energy Penetration Strengthened Using a Reversible Solid Oxide Cell Installed in a Building

Mario Lamagna and Davide Astiaso Garcia

***Abstract*—The renewable energy source (RES) penetration in end use must be strengthened to reach the prefixed decarbonization targets. A penetration obstacle is represented by the Power Grid, designed with an architecture disinclined to RES unpredictability. Nowadays, different solutions are available to integrate these latter issues without affecting the Grid, among these, the reversible Solid Oxide Cell (rSOC) promises high efficiencies and the possibility to control energy fluxes in both production and storage. In this study, a series of hourly simulations based on real data were designed to evaluate the rSOC capacity to integrate a large number of RESs in the end use of three different buildings, through analyzing the possible congestion on the Power Grid. As a rSOC model we chose the Smart Energy Hub proposed by Sylfen while for the buildings we selected a school, a hotel, and an office located in Procida, Italy. The results show the rSOC capacity to integrate RES increased from 40% to 62% according to the storage capacity and the building's hourly load curve and seasonal consumptions.**

***Index Terms*—Green hydrogen, RES integration, rSOC, power-to-power.**

I. Introduction

FACILITATING a Renewable Energy Source (RES) penetration in today's energy system is key to attaining decarbonization's target [1] as set by the different International Institutions [2]. Nonetheless, a high presence of connected non predictable RESs can represent a challenge to the actual energy systems [3].The integration of technologies able to ensure flexibility [4] and demand side management [5], i.e. able to cope with the misalliance between the production and the demand [6], can be a first attempt to sustain the RES penetration [7]. Nowadays, many different solutions are available [8], and a holistic approach is needed to understand how to integrate each one of them within the Power Grid to reach an optimized arrangement [9] while maintaining comfort targets for the final user [10].In order to achieve this future scenario with reliability, it is necessary to install technologies, such as storage systems [11] or solutions based on hydrogen, the so called Power-to-Gas (PtG) [12] or Power-to-X [13] hence able to work synergically with RES such as wind [14] and solar [15] energy, or with sustainable mobility [16], just to name a few. Currently, green hydrogen, which is produced starting from RES, is gaining momentum in multiple optimal solution [17], since it can be exploited in different end-uses with a positive decarbonization effect [18], especially in the hard to abate sectors [19]. Similarly, the building sector can benefit from PtG strategies [20], in this context, hydrogen can be used as an energy vector for storage purposes [21] or as a source for electricity and heating requirements [22].

Among the several different hydrogen technologies, the reversible Solid Oxide Cell (rSOC) is seen as a gamechanger, since it is unitized in one device which only requires a fuel cell (FC) and an electrolyzer (EC), thereby guaranteeing a storage and production capability in a compact space [23]. Additionally, its strong scalability and modularity, merged with its high efficiency, Combined Heat and Power (CHP), and fuel flexibility between hydrogen and natural gas (NG), make the rSOC an easy to adapt solution [24]. Sylfen [25], is manufacturing a compact rSOC solution designed for the building sector, converting the overproduction coming from the local RES into hydrogen that it will later be able to use by the same rSOC to produce electricity and heat when most needed, thus reducing the congestion on the Power Grid [26], and enhancing the building's sustainability and self-sufficiency [27]. These characteristics make the rSOC an interesting solution to be investigated to allow for RES penetration.

For this purpose, Specific Key Performance Indicators (KPIs) will be studied to evaluate the rSOC impact considering the varying RES availability, building end-use, and available storage capacity. From analyzing the obtained results in these different series of settings, an outlook on rSOC ability to integrate more RESs will emerge. The results obtained will represent an aggregated value to existing literature since most of the studies concerning this technology are focused on specific case studies or materials for manufacturing. In fact, the rSOC technology can be considered an innovative solution since until now few functioning systems were installed in a real environment as described in [28]–[30], while other manufacturers are getting close to the commercial phase. In this regard, Sylfen already tested its technology in a lab facility [31]. Other research was conducted to explore this field, in [32] a non-unitized FC and EC were studied in a dwelling house, although no comparisons were made with different end use buildings. A non-unitized solution was also

Manuscript received July 6, 2021; revised September 23, 2021; accepted October 12, 2021. Date of online publication February 14, 2022; date of current version February 24, 2021.

M. Lamagna is with Astronautical, Electrical and Energy Engineering Department (DIAEE), Sapienza University of Rome, Italy.

D. A. Garcia (corresponding author, email: davide.astiasogarcia@uniroma1.it; ORCID: https://orcid.org/0000-0003-0752-2146) is with Planning, Design, Technology of Architecture Department (DPDTA), Sapienza University of Rome, Italy.

DOI: 10.17775/CSEEJPES.2021.04920

studied in [33] and in [34] focusing on different RES coupling and building utilizations respectively. The rSOC use can be found in [35], nonetheless the authors used two different data references for the EC and FC models, combining them in a unitized system for the simulations, although they are not related, while in this study, a real rSOC will be simulated. Finally, the authors of this paper conducted a similar study in [36] but without exploring the effect of varying RES availability, end-use buildings and storage availability which represents a new contribution to this topic.

In this study, the primary objective is to understand how much of the local RES production can be integrated by means of a real rSOC, installed in real buildings. Simulations will be performed by means of ConfigDym, an inhouse software developed by Sylfen, and case studies will be used to analyze the energy needs of a school, an office, and a hotel located in Procida, Italy. These three buildings were selected because they are characterized by different hourly load curves throughout the day and different utilization factors throughout the year (seasonality) but have a similar annual consumption.

Since hydrogen use is determinable, especially for seasonal storage [37], the secondary objective of this research is to understand how the RES integration, by means of a rSOC system, is affected by the seasonality and load curves associated with different buildings, as well as their end-use and storage availability.

II. Materials and Method

In this section, information related to the investigated buildings and the used rSOC is provided. Additionally, the inputs and constraints imposed during the simulations and the adopted strategies to evaluate the research objectives will be described.

A. The Case Studies

Procida is a small island located in the south of Italy in the Naples's gulf and it is characterized by typical Mediterranean climate, with hot summers and mild winters. The three chosen buildings have an annual consumption of roughly 145 MWh each, although being differently distributed throughout the year. Moreover, the three building consumptions are totally electrified, with no gas usage. The data consumptions for the study cases were obtained through the local municipality and the local distribution system operator's cooperation.

1) Hotel

This facility is characterized by a strong seasonality, divided into three periods: i) Closing in December, ii) Opening for special events and maintenance in January, February, and November, iii) Normal functioning from March until October, with the peak attendance between June and August as can be seen in Figure 1.

Figure 2 shows the maximum and minimum values by month, and it can be determined how during summer vacation in Italy, i.e., from June to August, the hotel reaches its peak consumption, which is in line with the expected monthly producibility coming from a local photovoltaic (PV) system.

Nevertheless, going deeper into the details by analyzing the information reported in Figure 3, it can be determined that the peaks are recorded during the breakfast and dinner times, both periods characterized by a low PV production, which usually has its maximum during the lunch period between 12:00 and 13:00.

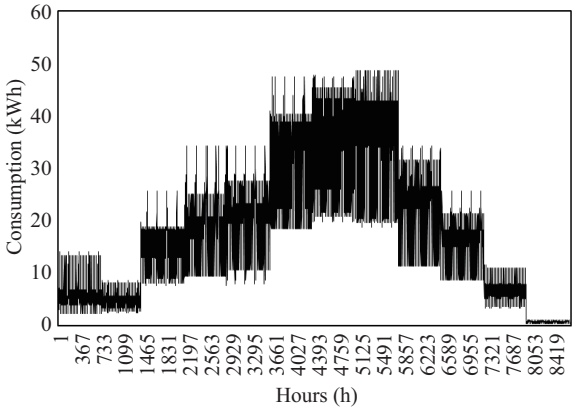

Fig. 1. Hotel annual electric consumption load shape.

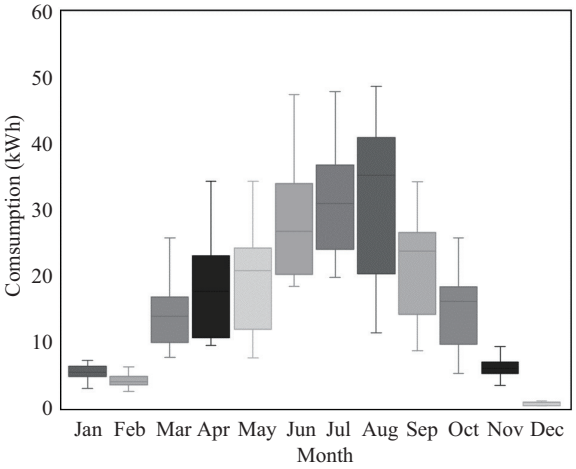

Fig. 2. Hotel monthly electric consumption.

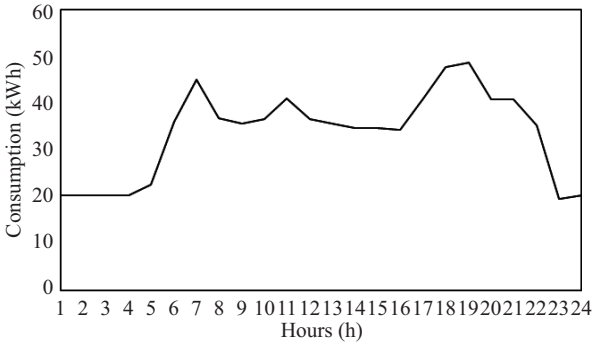

Fig. 3. Hotel's typical daily electric load shape.

This daily pattern, with different peak values, is noted throughout the year, since during the day the guests are spending their time outside the facility.

2) Office

The office is being used by the Municipality for different purposes, but outside some few special events hosted during the evening, the building is primarily used from 9:00 to 14:00,

while during the weekends, it is primarily closed. During the cold seasons, the consumption is higher primarily due to the heating system, which is based on electric stoves, while in summer a lower energy demand is recorded as shown in Figure 4.

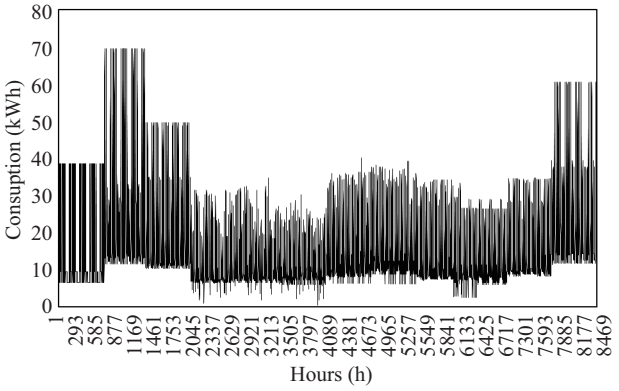

Fig. 4. Office annual electric consumption load shape.

Accordingly, in Figure 5, the peak values are recorded during February and December, while in January there was a problem with the datalogger controlled by the distributor system operator, which was unable to provide a result, only the mean consumption during the month.

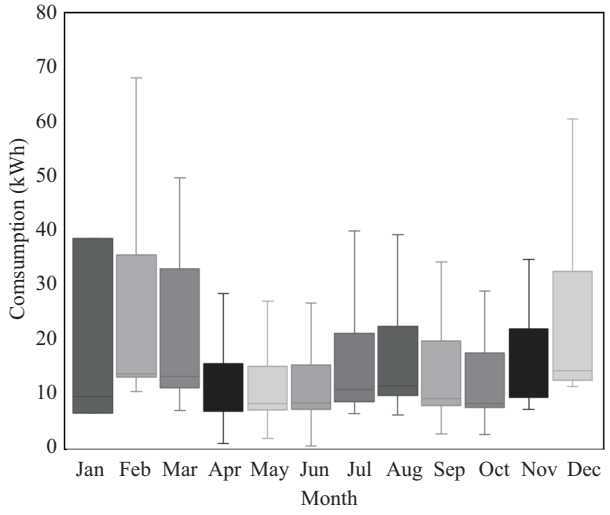

Fig. 5. Office monthly electric consumption.

Concerning the daily load shape, the curve has only one peak, as reported in Figure 6. Additionally, the consumption peak coincides with the production peak from a PV, but during the weekend and the evening hours, it could be recorded as a relevant overproduction, coming from the balance with lower consumptions.

3) School

In Italy, the school is interrupted during three different periods: i) from the 21st of December until the 7th of January, ii) one week during the Easter holidays, and iii) from June to September for the summer break. During this latter period, the school is closed, and the consumption is at a minimum as can be seen in Figure 7.

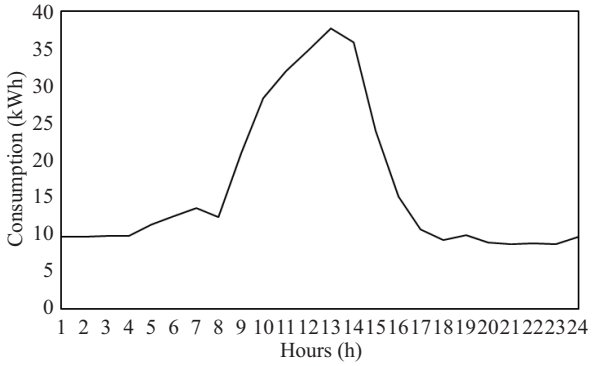

Fig. 6. Office typical daily electric load shape.

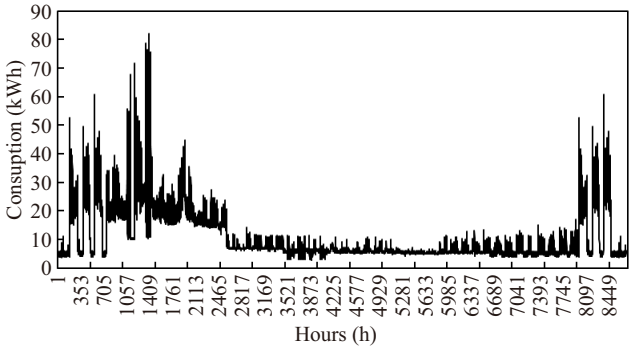

Fig. 7. School's annual electric consumption load shape.

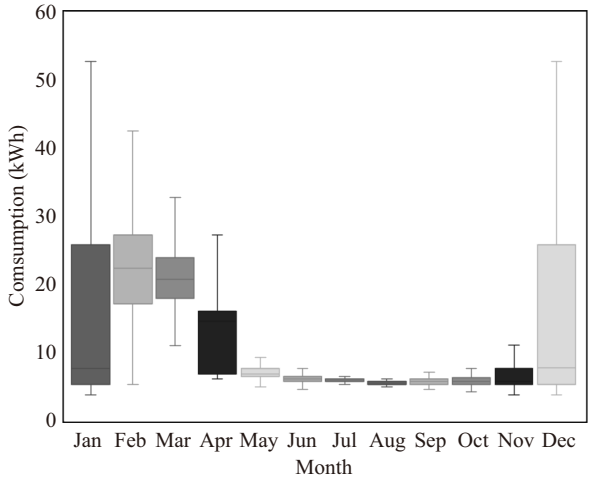

Fig. 8. School monthly electric consumption.

Also, in September, October, and November, due to the mild external temperatures, the consumption is also low.

The highest consumptions are recorded during the winter months, due to the heating system being based on heat pumps (HP).

Being different from the other case, the school's typical daily load shape reported in Figure 9 shows an on-and-off trend, due to the presence of autonomous heat pumps.

Along with a high load base, the school's load curve is characterized by several daily peaks, which follow the external temperature. Nevertheless, the bulk of demand is concentrated during the day's central hours.

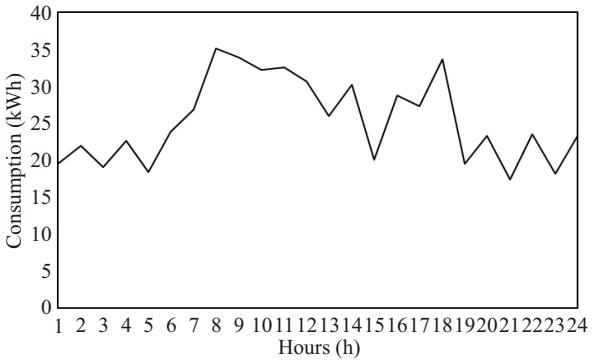

Fig. 9. School's typical daily electric load shape.

B. The rSOC

In this section, the information regarding the chosen energy system, its simulation software, and the boundary conditions imposed for this study are reported.

1) The Module

The module is based on the solution proposed by Sylfen, called the Smart Energy Hub (SEH).

The information reported in Table I refers to one SEH only, while it could be converted into a system of up to 6 working modules plus an additional lithium battery pack to cope with quick variations in the demand and production side. Additionally, this rSOC can work both with Natural Gas and hydrogen and in a CHP or connected with an HP or a domestic hot water (DHW) boiler. The SEH technical details and lab tests are available in [31].

TABLE I
RSOC FEATURES

Quantity	Unit	Value
EC power and compression	kW	9.9 – 40.8
EC efficiency	%	65–80
H_2production	Kg/h	0.25–0.9
Storage Pressure	Bar	200
FC Power	kW	6.7
FC consumption	Kg/h	0.4
FC efficiency	%	40–50

2) The Simulation Software

The simulation is performed by means of ConfigDym, based on MATLAB, whose functioning was already described by the authors in [36]. The rSOC can change its settings from EC to FC and vice versa in one hour steps in agreement with the new improved Switch Operation Restriction (SOR). The software will decide the working setting according to the energy balance between the building electric needs (BN) and PV production, i.e., a positive balance with PV overproduction and empty tank will activate the EC mode, otherwise the FC mode will operate. In the case of an empty or full tank, the system will interact with the Power Grid as usual, the software decision making strategy is summarized in Figure 10. Even if this is possible, no recurse to the NG or batteries will be allowed during the simulations to stress the PV production integration made exclusively by hydrogen and the rSOC.

3) Simulation Assumptions and KPIs

The simulations will last for one year with an hourly resolution, considering the installation of 1 module without any supplementary battery pack.

The primary research objective is to evaluate how the rSOC can integrate RES in a real building, and to do so as a starting point it will be simulated through the presence of a PV system able to cover 70% of the total energy demand, which is equal to 101, 5 MWh.

By means of PVWatts software [38], such a system is represented by a plant of 80 kWp in Procida. To determine the possible congestion on the grid or the RES integrable energy by the rSOC, a sensibility analysis is done in terms of PV and storage size. At first, simulations will be performed without the rSOC to define the reference scenario. Regarding the sensitivity analysis, the PV size will be increased starting from 80 kWp up to 160 kWp, with a 20% increase per step, thereby a total of five simulations.

Then the simulations will be performed with the rSOC to measure its effectiveness. Similarly, the storage will be increased to understand how much of its size affects the RES integration, and at the same time how the different end uses affect its importance. The initial tank is fixed at 100 kg of hydrogen with a 25% increase until 225 kg, for a total of 6 scenarios.

A simulation summary is reported in Figure 11, which shows 35 scenarios made for each building.

The initial tank size is chosen to cover five working day needs, which are assumed equal to 2000 kWh considering the 145 MWh annual consumption, the rSOC efficiency working in FC, and the hydrogen properties stored at 200 bars.

Additionally, from the simulations, it was necessary to exclude the possibility to use as fuel the NG when the tank is empty and the energy balance is negative, since in this paper the focus is to evaluate the RES penetration. Moreover, the possible heat recovery coming from the CHP mode will not be used in air preheating, as a more restrictive condition to evaluate the rSOC impact on the building energy balance. Finally, to understand how much the rSOC technology can help the RES penetration while reducing the possible congestion on the grid based on its flexibility, the following parameters will be extrapolated from the simulations and defined as KPIs:

- System Overproduction to Grid in kWh
- Hydrogen total production in Kg
- rSOC electric production in kWh
- Tank state of charge (SOC) greater than 70% of the total capacity in hours

III. RESULTS

The results obtained for each building in the 35 simulated scenarios will be presented in this section, divided into the three study cases. The values coming from the investigated KPIs will be discussed at the end of each paragraph, and they represent the cumulative value recorded during the annual simulation.

The tables have also a color indicator, starting from red for the worst performance up to dark green for the best result.

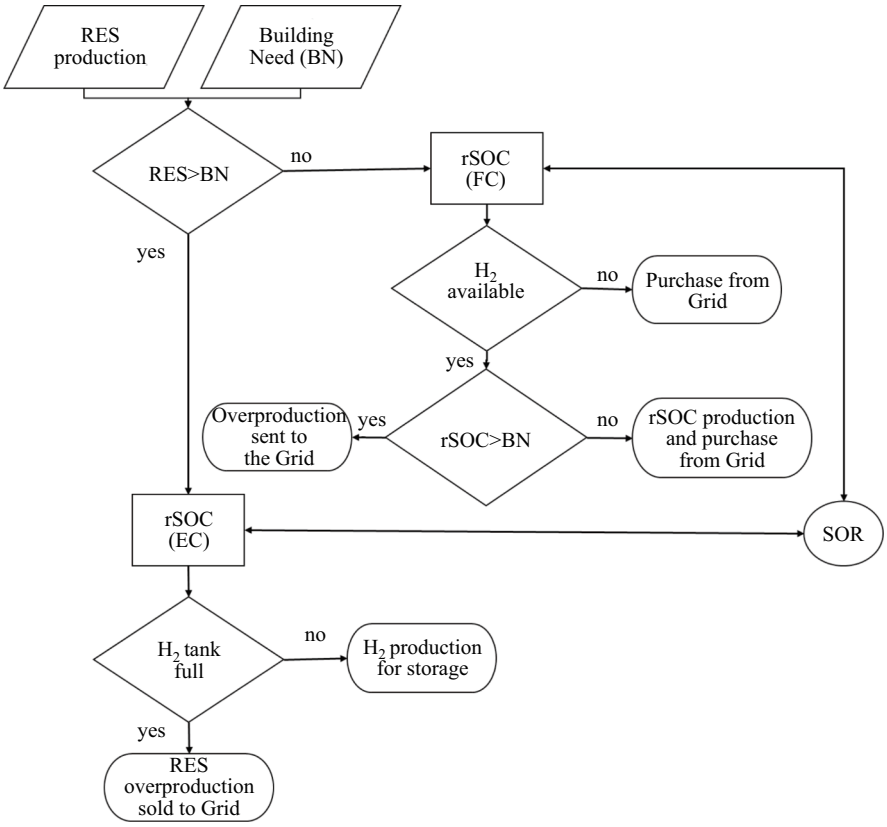

Fig. 10. Software synoptic.

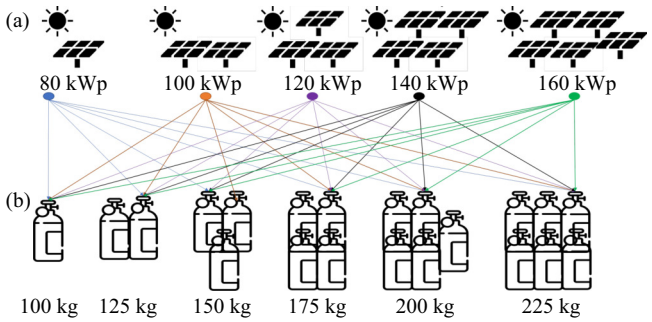

Fig. 11. (a) PV sizes studied and their combination with the storages. (b) Storage sizes studied.

The simulations with PV only, used as a reference scenario, are mentioned as PV only in Tables II, VI, and X.

A. Hotel

As identified in the previous section, the peak demand and the PV peak production are misaligned in this case, therefore the values concerning the overproduction are consistent throughout the year, and they are reported in Table II.

In this case a storage solution is indicated to save the PV surplus, in fact when considering the rSOC installation with a 100 kg tank, an overproduction reduction between 45% and 62% is recorded. When the rSOC is coupled with a 160 kWp PV it is roughly producing the same overproduction, i.e., congestion on the grid, of a 100 kWp PV plant.

Considering the first scenario (80 kWp, PV only), the annual overproduction exceeds 44% of the total PV production (101.5 MWh) but it is reduced to 27% with the rSOC.

TABLE II
OVERPRODUCTION RECORDED (KWH)

PV Storage	80 kWp	100 kWp	120 kWp	140 kWp	160 kWp
PV only	44,630	67,690	91,630	116,090	140,890
100 kg	27,855	33,211	41,715	53,844	69,886
125 kg	27,855	33,211	41,715	53,844	69,886
150 kg	27,855	33,211	41,715	53,844	69,886
175 kg	27,855	33,211	41,715	53,844	69,886
200 kg	27,855	33,211	41,715	53,844	69,886
225 kg	27,855	33,211	41,715	53,844	69,886

Considering Table III, which displays the annual hydrogen produced in EC mode, the PV size influence can be recognized, while storage capacity does not affect the result. This means that the EC mode could be activated each time when needed, with the only exception being the case of the 100 kg storage and 160 kWp PV when the tank was full.

TABLE III
HYDROGEN PRODUCED (KG)

PV Storage	80 kWp	100 kWp	120 kWp	140 kWp	160 kWp
100 kg	640	1,015	1,342	1,617	1,804
125 kg	640	1,015	1,342	1,617	1,817
150 kg	640	1,015	1,342	1,617	1,817
175 kg	640	1,015	1,342	1,617	1,817
200 kg	640	1,015	1,342	1,617	1,817
225 kg	640	1,015	1,342	1,617	1,817

Therefore, it is not a surprise that the electricity produced by the rSOC, reported in Table IV, is just varying according

TABLE IV
RSOC ELECTRICITY PRODUCTION (KWH)

PV Storage	80 kWp	100 kWp	120 kWp	140 kWp	160 kWp
100 kg	5,052	10,883	16,048	19,745	21,799
125 kg	5,052	10,883	16,048	19,745	21,817
150 kg	5,052	10,883	16,048	19,745	21,817
175 kg	5,052	10,883	16,048	19,745	21,817
200 kg	5,052	10,883	16,048	19,745	21,817
225 kg	5,052	10,883	16,048	19,745	21,817

to the PV variation which leads to a 54% increase for the first simulation step and 32%, 19% and 9% increases in accordance with the subsequent increments. The resulting flattened values are attributable to the fewer hours with a negative balance, namely the balance between RES production and building needs, which trigger the FC mode.

If the focus is shifted on the tank SOC, it is possible to notice in Table V that the storage of SOC is greater than its 70% capacity, which is reached for less than 3000 h, i.e., 32% of the time in the worst-case scenario.

TABLE V
TANK SOC GREATER THAN 70% OF TOTAL CAPACITY (H)

PV Storage	80 kWp	100 kWp	120 kWp	140 kWp	160 kWp
100 kg	–	–	–	130	2,832
125 kg	–	–	–	–	2,452
150 kg	–	–	–	–	307
175 kg	–	–	–	–	–
200 kg	–	–	–	–	–
225 kg	–	–	–	–	–

Figure 12 shows the SOC annual trend for the 100 kg tank, and it is possible to determine for the 160 kWp PV plant that the storage reaches its maximum capacity in the summertime with the maximum PV production, and again at the end of the year, when the hotel is closed.

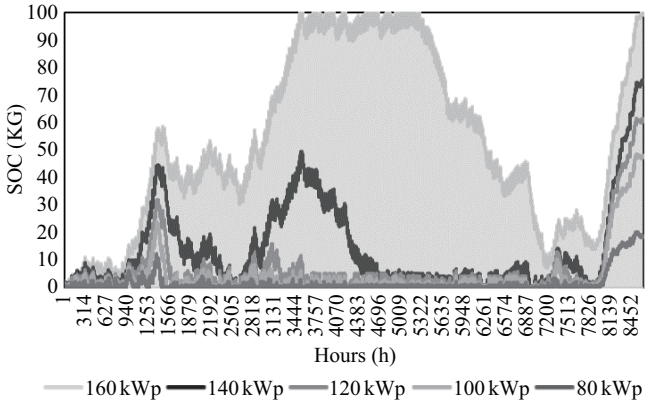

Fig. 12. Hotel tank SOC trend varying the PV size maintaining its capacity at 100 kg.

Otherwise, the SOC never reaches its maximum capacity in the other remaining case with lower PV power.

B. Office

The office load curve, different from the previous case, has a good coincidence between building peak demand and PV production. In fact, in Table VI it shows a 34% overproduction in the scenario with only PV, while it decreases to 20% with the rSOC. Therefore, this situation reflects a higher direct consumption of PV production.

TABLE VI
OVERPRODUCTION RECORDED (KWH)

PV Storage	80 kWp	100 kWp	120 kWp	140 kWp	160 kWp
PV only	34,920	55,740	77,860	101,110	125,020
100 kg	20,963	27,727	33,856	50,345	70,121
125 kg	20,963	27,727	33,856	49,231	68,989
150 kg	20,963	27,727	33,856	48,163	67,839
175 kg	20,963	27,727	33,856	47,013	66,740
200 kg	20,963	27,727	33,856	45,879	65,551
225 kg	20,963	27,727	33,856	45,879	64,353

Since the available surplus to produce hydrogen decreases, consequently the produced hydrogen quantity is reduced as reported in Table VII. For the two cases with greater PV, the production changes also according to the storage size, implying that the maximum SOC was reached.

TABLE VII
HYDROGEN PRODUCED (KG)

PV Storage	80 kWp	100 kWp	120 kWp	140 kWp	160 kWp
100 kg	498	793	1,148	1,289	1,369
125 kg	498	793	1,148	1,318	1,397
150 kg	498	793	1,148	1,345	1,425
175 kg	498	793	1,148	1,375	1,452
200 kg	498	793	1,148	1,405	1,480
225 kg	498	793	1,148	1,405	1,509

Less available hydrogen means also less rSOC production. Table VIII shows the reported electricity production for each scenario, in which the 160 kWp and 140 kWp cases recorded a 2% increase every time the tank increased by 25%. As noted, increasing the PV size greatly affects the rSOC outputs. The change from 80 kWP to 100 kWP indicates a 47% electricity increase, while the subsequent 20% increases lead to a 38%, 15% and 8% rise respectively.

TABLE VIII
RSOC ELECTRICITY PRODUCTION (KWH)

PV Storage	80 kWp	100 kWp	120 kWp	140 kWp	160 kWp
100 kg	4,601	8,743	14,100	16,625	18,198
125 kg	4,601	8,743	14,100	16,988	18,564
150 kg	4,601	8,743	14,100	17,328	18,965
175 kg	4,601	8,743	14,100	17,689	19,311
200 kg	4,601	8,743	14,100	18,074	19,721
225 kg	4,601	8,743	14,100	18,074	20,123

Table IX shows the hours spent by the tank in a SOC greater than 70% of its total capacity.

TABLE IX
TANK SOC GREATER THAN 70% OF TOTAL CAPACITY (H)

PV Storage	80 kWp	100 kWp	120 kWp	140 kWp	160 kWp
100 kg	–	–	1,197	2,519	3,132
125 kg	–	–	14	2,419	3,226
150 kg	–	–	–	2,325	3,289
175 kg	–	–	–	2,193	3,197
200 kg	–	–	–	2,092	3,098
225 kg	–	–	–	1,723	2,989

The tank reaches its full capacity in both 160 kWp and 140 kWp cases, as can be seen in Figure 13. The trends show how the system stores energy during the summer and uses it

until the end of November. During the other months the PV overproduction is not sufficient to trigger the EC mode.

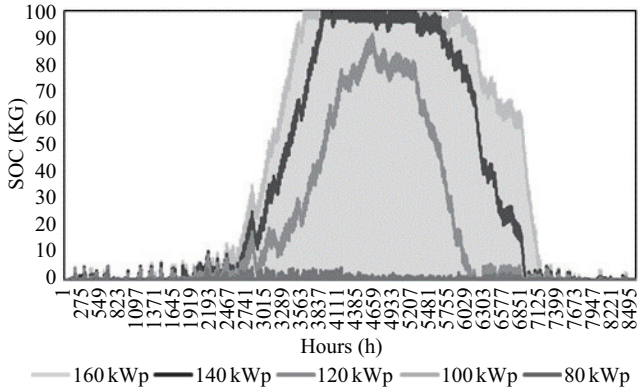

Fig. 13. Office tank SOC trend varying the PV size maintaining its capacity at 100 kg.

Indeed, installing larger tanks will guarantee longer storage periods during summer, with subsequent longer production during autumn and winter when the heating system is on and the PV production is at its minimum.

C. School

The school is the building among the three analyzed with the longest inactive period. Table X shows the overproduction recorded at different PV and tank sizes. The 80 kWp PV overproduction reaches 63% without storage and decreases to 18% when the rSOC system is installed. The school is the building where the rSOC contribution is more evident in terms of RES integration among the analyzed cases.

TABLE X
OVERPRODUCTION RECORDED (KWH)

PV Storage	80 kWp	100 kWp	120 kWp	140 kWp	160 kWp
PV only	64,180	86,140	108,920	132,360	156,360
100 kg	18,600	36,817	56,389	76,939	98,321
125 kg	17,490	35,682	55,237	75,793	97,207
150 kg	16,461	34,460	54,112	74,627	96,050
175 kg	15,313	33,273	53,001	73,587	94,943
200 kg	14,143	32,133	51,838	72,383	93,709
225 kg	13,361	30,986	50,705	71,329	92,534

Thanks to the rSOC, the overproduction of a 160 kWp PV plant is similar to a 110 kWp plant, therefore allowing for integration less impact with a system 45% bigger.

Table XI shows the hydrogen produced, which increases for the increasing PV and storage size, underlying the fact that in all cases the maximum SOC is reached, therefore five days of storage is underestimated for the building necessities, and a larger one should be considered for the installation.

TABLE XI
HYDROGEN PRODUCED (KG)

PV Storage	80 kWp	100 kWp	120 kWp	140 kWp	160 kWp
100 kg	1,109	1,192	1,262	1,332	1,393
125 kg	1,137	1,220	1,290	1,359	1,419
150 kg	1,162	1,249	1,314	1,388	1,447
175 kg	1,190	1,276	1,343	1,413	1,472
200 kg	1,220	1,302	1,370	1,442	1,502
225 kg	1,240	1,329	1,397	1,466	1,531

Due to the high hydrogen availability, especially at the end of the summer after the closing period, the rSOC can produce high amounts of electricity covering from 8% up to 15% of the total electric demand as can been identified from Table XII. Similar to the office case, a 25% storage size increase leads to a 2% increase of electric production, while a 20% PV increment leads to a smaller increase of between 4% and 8% when compared with the previous buildings.

TABLE XII
RSOC ELECTRICITY PRODUCTION (KWH)

PV Storage	80 kWp	100 kWp	120 kWp	140 kWp	160 kWp
100 kg	16,329	17,452	18,706	19,788	20,772
125 kg	16,685	17,910	19,107	20,210	21,138
150 kg	17,037	18,320	19,535	20,574	21,543
175 kg	17,436	18,744	19,912	20,990	21,942
200 kg	17,485	19,128	20,339	21,380	22,369
225 kg	18,102	19,540	20,728	21,787	22,756

Nevertheless, the periods elapsed when the SOC exceeds 70% of total capacity, shown in Table XIII, are the higher among all the simulated scenarios. These conditions are attributable to the three months summer break, when the PV productions is at its maximum and the energy balance can trigger the EC mode.

TABLE XIII
TANK SOC GREATER THAN 70% OF TOTAL CAPACITY (H)

PV Storage	80 kWp	100 kWp	120 kWp	140 kWp	160 kWp
100 kg	2,724	3,528	3,994	4,260	4,493
125 kg	2,567	3,516	3,870	4,130	4,397
150 kg	2,459	3,469	3,858	4,126	4,324
175 kg	2,310	3,353	3,782	4,086	4,288
200 kg	2,197	3,234	3,769	4,029	4,254
225 kg	1,999	3,177	3,678	3,967	4,216

Figure 14 shows the tank SOC curve maintaining its size fixed at 100 kg while increasing the PV installed power.

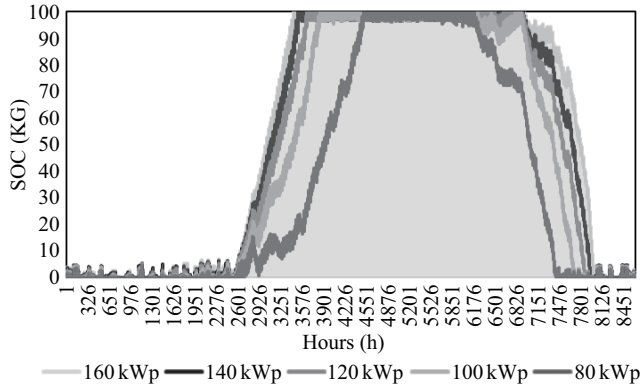

Fig. 14. School tank SOC trend varying the PV size maintaining its capacity at 100 kg.

The figure shows a charging trend during the spring and summer months and a discharging behavior starting from September when schools start up again. The larger the PV installed, the earlier the tank will be filled.

Since in each scenario the maximum SOC was reached, it is interesting to analyze the SOC curve at the fixed PV power with varying tank capacity. Figure 15 shows this latter

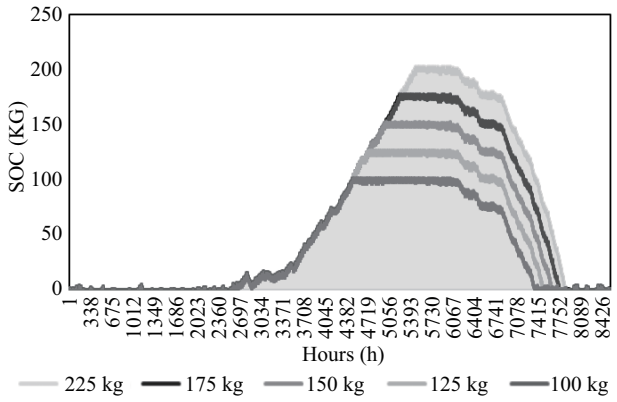

Fig. 15. School tank SOC trend varying the storage size maintaining the PV at 80 kWp.

information. Also in this case, five distinctive trends can be deduced: i) quick SOC fluctuations when the school is open at the curve extremes, ii) a charging profile during spring, iii) a flat profile during summer when the tank is full and the school is closed, iv) a discharging profile at the beginning of the academic year with mild temperatures, and v) a more intense discharging slope while the school is open and the PV production begins to decrease during the winter.

IV. Conclusion

We can identify from the presented tables and figures how much each scenario can differ from one to another while still using the same technology. Although starting from a comparable annual consumption, the different hourly load curves, related to the building's end uses, greatly influenced the results, which were analogous but nonetheless dissimilar, confirming the importance of the secondary objective of this paper.

As matter of fact, for the school, being different from the office and hotel, the PV increasing is less effective since this is the case with an already large surplus and rSOC production. This condition is attributable to the overproduction primarily recorded when the school is closed for three consecutive months, therefore the lower consumption has a greater effect than a greater overproduction, showing how the load curve interacts with the outputs. A similar behavior is recorded for the hotel at the end of the year when it is closed, compared with the office during the summer.

Considering the specific climate conditions, the three cases reach the tank maximum capacity during August, while the hotel is the only one to have a second peak in December, when it is closed and can store the available overproduction.

However, all the obtained results converge on rSOC effectiveness, reducing the local RES excess and the relative pressure on the Power Grid. Similarly, the rSOC was able to integrate in all the cases a greater quantity of RES and at the same time to produce electricity on its own, thereby reducing the demand from the Power Grid and its congestion. The RES penetration is fostered by this technology being able to give flexibility to the demand and production sides in a building as identified as the primary objective of this study. While considering a PV installation, the rSOC presents the pathway to the present system at least 40% larger without affecting the grid, thereby assuring better performances and autonomy.

Acknowledgment

This research has been carried out under the project "L'idrogeno verde nei contesti insulari coinvolgendo le Municipalità" funded by Sapienza University of Rome.

References

[1] A. Bhuvanesh, S. T. Jaya Christa, S. Kannan, and M. Karuppasamy Pandiyan, "Aiming towards pollution free future by high penetration of renewable energy sources in electricity generation expansion planning," *Futures*, vol. 104, pp. 25–36, Dec. 2018, doi: 10.1016/j.futures.2018.07.002.

[2] The European Green Deal (2019), European Commission, Communication from the Commission.

[3] S. Impram, S. V. Nese, and B. Oral, "Challenges of renewable energy penetration on power system flexibility: A survey," *Energy Strategy Reviews*, vol. 31, pp. 100539, Sep. 2020, doi: 10.1016/j.esr.2020.100539.

[4] F. Mancini, J. Cimaglia, G. Lo Basso, and S. Romano, "Implementation and simulation of real load shifting scenarios based on a flexibility price market strategy–the Italian residential sector as a case study," *Energies*, vol. 14, no. 11, pp. 3080, May 2021, doi: 10.3390/en14113080.

[5] D. Groppi, A. Pfeifer, D. Astiaso Garcia, G. Krajačić, and N. Duić, "A review on energy storage and demand side management solutions in smart energy islands," *Renewable and Sustainable Energy Reviews*, vol. 135, pp. 110183, Jan. 2021, doi: 10.1016/j.rser.2020.110183.

[6] G. Pulazza, N. Zhang, C. Q. Kang, and C. A. Nucci, "Expansion planning model coordinated with both stationary and transportable storage systems for transmission networks with High RES penetration," in *2020 IEEE International Conference on Environment and Electrical Engineering and 2020 IEEE Industrial and Commercial Power Systems Europe* (*EEEIC/I&CPS Europe*), *2020*, pp. 1–6, doi: 10.1109/EEEIC/ICPSEurope49358.2020.9160801.

[7] S. X. Zhang, H. Z. Cheng, D. Wang, L. B. Zhang, F. R. Li, and L. Z. Yao, "Distributed generation planning in active distribution network considering demand side management and network reconfiguration," *Applied Energy*, vol. 228, pp. 1921–1936, Oct. 2018, doi: 10.1016/j.apenergy.2018.07.054.

[8] B. Mohandes, M. S. E. Moursi, N. Hatziargyriou, and S. E. Khatib, "A Review of power system flexibility with high penetration of renewables," *IEEE Transactions on Power Systems*, vol. 34, no. 4, pp. 3140–3155, Jul. 2019, doi: 10.1109/TPWRS.2019.2897727.

[9] W. You, Y. Geng, H. J. Dong, J. Wilson, H. Y. Pan, R. Wu, L. Sun, X. Zhang, and Z. Q. Liu, "Technical and economic assessment of RES penetration by modelling China's existing energy system," *Energy*, vol. 165, pp. 900–910, Dec. 2018, doi: 10.1016/j.energy.2018.10.043.

[10] F. Mancini, F. Nardecchia, D. Groppi, F. Ruperto, and C. Romeo, "Indoor environmental quality analysis for optimizing energy consumptions varying air ventilation rates," *Sustainability*, vol. 12, no. 2, pp. 482, Jan. 2020, doi: 10.3390/su12020482.

[11] M. Peker, A. S. Kocaman, and B. Y. Kara, "Benefits of transmission switching and energy storage in power systems with high renewable energy penetration," *Applied Energy*, vol. 228, pp. 1182–1197, Oct. 2018, doi: 10.1016/j.apenergy.2018.07.008.

[12] B. Nastasi, S. Mazzoni, D. Groppi, A. Romagnoli, and D. Astiaso Garcia, "Solar power-to-gas application to an island energy system," *Renewable Energy*, vol. 164, pp. 1005–1016, Feb. 2021, doi: 10.1016/j.renene.2020.10.055.

[13] M. Robinius et al., "Power-to-hydrogen and hydrogen-to-X: Which markets? Which economic potential? Answers from the literature," 2017 14th International Conference on the European Energy Market (EEM), 2017, pp. 1–6, doi: 10.1109/EEM.2017.7981884.

[14] X. Wu, H. Li, X. Wang and W. Zhao, "Cooperative Operation for Wind Turbines and Hydrogen Fueling Stations With On-Site Hydrogen Production," in IEEE Transactions on Sustainable Energy, vol. 11, no. 4, pp. 2775–2789, Oct. 2020, doi: 10.1109/TSTE.2020.2975609.

[15] R. Boudries and A. Khellaf, "Techno-economic study of solar electrolytic hydrogen production at high temperature," 2020 6th International Symposium on New and Renewable Energy (SIENR), 2021, pp. 1–5, doi: 10.1109/SIENR50924.2021.9631906.

[16] G. Li, J. Chen, X. Zheng, C. Xiao and S. Zhou, "Research on Energy Management Strategy of Hydrogen Fuel Cell Vehicles," 2020 Chinese Automation Congress (CAC), 2020, pp. 7604–7607, doi: 10.1109/CAC51589.2020.9326669.
[17] J. R. Li, J. Lin, H. C. Zhang, Y. H. Song, G. Chen, L. J. Ding, and D. X. Liang, "Optimal investment of electrolyzers and seasonal storages in hydrogen supply chains incorporated with renewable electric networks," *IEEE Transactions on Sustainable Energy*, vol. 11, no. 3, pp. 1773–1784, Jul. 2020, doi: 10.1109/TSTE.2019.2940604.
[18] B. Nastasi, "Hydrogen policy, market, and R&D project," in *Solar Hydrogen Production*, Cambridge, MA, USA: Elsevier, 2019, doi: 10.1016/B978-0-12-814853-2.00002-3.
[19] M. Schulthoff, I. Rudnick, A. Bose, and E. Gençer, "Role of hydrogen in a low-carbon electric power system: a case study," *Frontiers in Energy Research*, vol. 8, pp. 585461, Jan. 2021, doi: 10.3389/fenrg.2020.585461.
[20] B. Nastasi and U. Di Matteo, "Innovative use of hydrogen in energy retrofitting of listed buildings," *Energy Procedia*, vol. 111, pp. 435–441, Mar. 2017, doi: 10.1016/j.egypro.2017.03.205.
[21] B. Nastasi, S. Mazzoni, D. Groppi, A. Romagnoli, and D. Astiaso Garcia, "Optimized integration of Hydrogen technologies in Island energy systems," *Renewable Energy*, vol. 174, pp. 850–864, Aug. 2021, doi: 10.1016/j.renene.2021.04.137.
[22] C. Fu, J. Lin, Y. H. Song, Y. Zhou, and S. J. Mu, "Model predictive control of an integrated energy microgrid combining power to heat and hydrogen," in *2017 IEEE Conference on Energy Internet and Energy System Integration* (*EI2*), 2017, pp. 1–6, doi: 10.1109/EI2.2017.8245756.
[23] X. T. Xing, J. Lin, Y. H. Song, Q. Hu, Y. Zhou, and S. J. Mu, "Optimization of hydrogen yield of a high-temperature electrolysis system with coordinated temperature and feed factors at various loading conditions: A model-based study," *Applied Energy*, vol. 232, pp. 368–385, Dec. 2018, doi: 10.1016/j.apenergy.2018.09.020.
[24] X. T. Xing, J. Lin, Y. H. Song, J. Song, and S. J. Mu, "Intermodule management within a large-capacity high-temperature power-to-hydrogen plant," *IEEE Transactions on Energy Conversion*, vol. 35, no. 3, pp. 1432–1442, Sep. 2020, doi: 10.1109/TEC.2020.2978552.
[25] Sylfen. (2016, Nov.). Energy is at the heart of human civilisation. Available: https://sylfen.com/en/home/
[26] M. Greiml, F. Fritz, and T. Kienberger, "Increasing installable photovoltaic power by implementing power-to-gas as electricity grid relief–A techno-economic assessment," *Energy*, vol. 235, pp. 121307, Nov. 2021, doi: 10.1016/j.energy.2021.121307.
[27] D. Groppi, D. Astiaso Garcia, G. Lo Basso, F. Cumo, and L. De Santoli, "Analysing economic and environmental sustainability related to the use of battery and hydrogen energy storages for increasing the energy independence of small islands," *Energy Conversion and Management*, vol. 177, pp. 64–76, Dec. 2018, doi: 10.1016/j.enconman.2018.09.063.
[28] J. Mermelstein and O. Posdziech, "Development and demonstration of a novel reversible SOFC system for utility and micro grid energy storage," *Fuel Cells*, vol. 17, no. 4, pp. 562–570, Aug. 2017, doi: 10.1002/fuce.201600185.
[29] O. Posdziech, K. Schwarze, and J. Brabandt, "Efficient hydrogen production for industry and electricity storage via high-temperature electrolysis," *International Journal of Hydrogen Energy*, vol. 44, no. 35, pp. 19089–19101, Jul. 2019, doi: 10.1016/j.ijhydene.2018.05.169.
[30] R. Peters, M. Frank, W. Tiedemann, I. Hoven, R. Deja, N. Kruse, Q. Fang, L. Blum, and R. Peters, "Long-term experience with a 5/15kW-class reversible solid oxide cell system," *Journal of the Electrochemical Society*, vol. 168, no. 1, pp. 014508, Jan. 2021, doi: 10.1149/1945-7111/abdc79.
[31] A. Nechache and S. Hody, "Test and evaluation of an hybrid storage solution for buildings, based on a reversible high-temperature electrolyzer," *ECS Transactions*, vol. 91, no. 1, pp. 2485–2494, Jul. 2019, doi: 10.1149/09101.2485ecst.
[32] Í. Martín-García, E. Rosales-Asensio, A. González-Martínez, S. Bracco, F. Delfino, and M. De Simón-martín, "Hydrogen as an energy vector to optimize the energy exploitation of a self-consumption solar photovoltaic facility in a dwelling house," *Energy Reports*, vol. 6, no. S3, pp. 155–166, Feb. 2020, doi: 10.1016/j.egyr.2019.10.034.
[33] C. Marino, A. Nucara, M. Pietrafesa, and A. Pudano, "An energy self-sufficient public building using integrated renewable sources and hydrogen storage," *Energy*, vol. 57, pp. 95–105, Aug. 2013, doi: 10.1016/j.energy.2013.01.053.
[34] H. Mehrjerdi, "Peer-to-peer home energy management incorporating hydrogen storage system and solar generating units," *Renewable Energy*, vol. 156, pp. 183–192, Aug. 2020, doi: 10.1016/j.renene.2020.04.090.
[35] M. D. Mukelabai, J. M. Gillard, and K. Patchigolla, "A novel integration of a green power-to-ammonia to power system: Reversible solid oxide fuel cell for hydrogen and power production coupled with an ammonia synthesis unit," *International Journal of Hydrogen Energy*, vol. 46, no. 35, pp. 18546–18556, May 2021, doi: 10.1016/j.ijhydene.2021.02.218.
[36] M. Lamagna, B. Nastasi, D. Groppi, C. Rozain, M. Manfren, and D. Astiaso Garcia, "Techno-economic assessment of reversible Solid Oxide Cell integration to renewable energy systems at building and district scale," *Energy Conversion and Management*, vol. 235, pp. 113993, May 2021, doi: 10.1016/j.enconman.2021.113993.
[37] G. S. Pan, W. Gu, Y. P. Lu, H. F. Qiu, S. Lu, and S. Yao, "Optimal planning for electricity-hydrogen integrated energy system considering power to hydrogen and heat and seasonal storage," *IEEE Transactions on Sustainable Energy*, vol. 11, no. 4, pp. 2662–2676, Oct. 2020, doi: 10.1109/TSTE.2020.2970078.
[38] PVWatts website. [Online]. National Laboratory of the U.S. Department of Energy. Available: https://pvwatts.nrel.gov/

Mario Lamagna is a Ph.D. candidate in Applied Physics, his research is focused primarily on hydrogen application in buildings. He actively works in European projects (Horizon 2020, Interreg MED) and national research projects in the field of renewable energies and smart energy systems. He is the founder of a Start-Up (LIF Energy) dedicate to feasibility studies on green hydrogen production.

Davide Astiaso Garcia is Professor of Thermal Sciences, Energy Technology and Building Physics at Sapienza University of Rome. His full operating skills include, among others: Renewable energies, smart energy systems, energy efficiency in buildings, energy modelling, energy forecasting, environmental impact assessments, pollution risk management, indoor and outdoor air quality monitoring and mitigation measures. Furthermore, he is the Secretary General of the Italian Wind Energy Association (ANEV). He has participated in more than 15 European (Horizon 2020, Interreg Med, ENPI CBC Med, Erasmus+) and national research projects in the field of renewable energies and smart energy systems (in many cases as Principal Investigator and Project Coordinator).